

d^0 Ferromagnetism in Ag-doped Monoclinic ZrO₂ Compounds

L. Chouhan¹, G. Bouzerar² and S. K. Srivastava^{1*}

¹Department of Physics, Central Institute of Technology Kokrajhar, Kokrajhar-783370, India

²CNRS et Université Claude Bernard Lyon 1, F-69622, Lyon, France

*Corresponding Author E-mail: sk.srivastava@cit.ac.in

Abstract

Recently d^0 or intrinsic ferromagnetism was believed to provide an alternative pathway to transition metal induced ferromagnetism in oxide. In pursuit of augmenting the area of d^0 ferromagnetism; we have undertaken to study the crystal structure and magnetic properties of Ag-doped ZrO₂ compounds. Polycrystalline samples of Zr_{1-x}Ag_xO₂ (with x=0, 0.02, 0.04, 0.06 and 0.08) were prepared by solid-state reaction route. All the prepared compounds are found to crystallize in monoclinic symmetry of ZrO₂. In our study, pure ZrO₂ compound exhibits paramagnetic behavior. However, the Ag-doped ZrO₂ compounds exhibit ferromagnetic to paramagnetic transition. The Curie temperature (θ_c) was found to increase from 28.7 K for x=0.02 to 173.2 K for x= 0.08 doped ZrO₂. Thus, the introduction of Ag in ZrO₂ induces ferromagnetism with a large θ_c . The measurements of hysteresis curves indicate that Ag doped ZrO₂ compounds exhibit hysteresis loops with a coercivity of around 1350 Oe. Moreover, increase in Ag concentration resulted increase in the value of saturation magnetization (M_s); the maximum value of M_s was recorded as 0.01 μ_B /Ag ion for x= 0.06 sample. The sintering of sample at high temperature (1350^oC) diminishes the ferromagnetism and it leads to paramagnetic behaviour.

Key Words: Monoclinic ZrO₂; Ag-doping; d^0 Ferromagnetism; Defect Induced Magnetism

1. Introduction:

Over last couple of decades, there has been persistent effort by researchers to explore new materials which can be integrated for spintronics devices, such as giant magneto-resistance sensors, magneto-resistive random-access memories and storage media [1]. Spintronics devices, where both charge as well as spin are utilized, have been projected to have plenty of advantages over prevalent semiconductor devices, such as faster data processing, non-volatility, low power consumption and increased storage density [1, 2]. Among the various explored materials for spintronics devices, transition metal (TM) doped semiconducting oxide materials were studied extensively. Many TM-doped oxides, such as ZnO, SnO₂ and TiO₂ have been reported to exhibit room temperature ferromagnetism (RTFM) [3-11]. The magnetic coupling through exchange interaction of delocalized 3d electrons via structural defects (oxygen vacancies, V_o) has been put forward as possible explanation of the ferromagnetism observed in TM-doped oxides [10]. Although, the experimental search for ferromagnetism (FM) in TM-doped oxide materials has been continued to be dogged, but it has not yet resulted in reproducible and homogeneous magnetic materials and there is a debate whether RTFM is intrinsic or due to the magnetic ion cluster [11-13].

In order to get a clean material exhibiting RTFM, several other types of materials were studied and explored. In addition to TM-doped oxide materials, unexpected ferromagnetism has been reported or predicted in several pure oxides like HfO₂, CaO, ZnO, ZrO₂, TiO₂, MgO, SnO₂ and, even in CaB₆ [14-20]. Such unexpected ferromagnetism was termed as d^0 ferromagnetism or intrinsic ferromagnets i.e. the materials that do not contain magnetic impurities. Thus, the d^0 or intrinsic ferromagnetism was believed to provide an alternative pathway to TM-induced ferromagnetism. The origin of the magnetism in these materials was considered due to point defects such as cation vacancies, which induces a local magnetic moment on the neighboring oxygen atoms [15, 20]. To circumvent the difficulties of defect control, an alternative way, which consists of the substitution of non-magnetic elements in dioxides such as AO₂ (A=Ti, Zr, or Hf), was proposed [21]. Following to this idea, many *ab-initio* studies have predicted ferromagnetism with high Curie Temperature (θ_c) in several non-magnetic elements doped oxides, such as K-SnO₂ [22], Ag-SnO₂ [23], Mg-SnO₂ [24], anatase Li-TiO₂ [25], rutile K-TiO₂ [26], V-TiO₂ [27], K-ZrO₂ [16, 26]. Experimentally, d^0 magnetism were observed in several non-magnetic elements doped oxides such as; alkali metal doped ZnO [28-30]; Cu doped TiO₂ prepared in thin film form [31, 32], C-doped TiO₂

prepared by solid state route [33], K-SnO₂ [34], Li-SnO₂ [35], K-TiO₂ [36], Cu-ZnO [37] and Na-SnO₂ [38].

Recently Zirconium dioxide (ZrO₂) was projected as one of the promising candidates exhibiting d^0 ferromagnetism. ZrO₂ is a multipurpose material used in various scientific & technological applications due to its high dielectric constant, ionic conductivity, wide optical band gap, high chemical and thermal stabilities, low optical loss and high transparency [39-41]. It can crystallize in three different forms i.e. monoclinic (space group: P2₁/c), tetragonal (space group: P4₂/nmc) and cubic (space group: Fm3m) structures [39-40]. The monoclinic phase of zirconia is usually thermodynamically stable up to 1400 K. The tetragonal and cubic phases of ZrO₂ can be stabilized either by heating at very high temperature (1480 < T < 2650 K for tetragonal phase and, T > 2650 K for cubic phase) or by the addition of another cation such as Ca²⁺ or Y³⁺ [40]. In fact, several recent reports indicate that pure ZrO₂ exhibits room temperature d^0 ferromagnetism and it is related to the presence of oxygen vacancies or structural defects. Some of these studies also show that the crystallographic phase is very important in this context, with reports of ferromagnetism more common for tetragonal ZrO₂ structures [42-44]. The theoretical studies predicted high-temperature ferromagnetism in TM-doped cubic zirconia [45] as well as non-magnetic element doped zirconia such as K [16, 26] and V [46] in ZrO₂. However, it was predicted that doping with Cu [47], Cr [45] or Ca [16] in ZrO₂ can result in paramagnetism, antiferromagnetic or non-magnetic ground states, respectively.

Although, Ag-doped ZrO₂ was attempted by researchers for different kind of application such as in resistive switching, soot oxidation and opto-electronics [48-50] but, there exists no report on study of magnetic properties of Ag-doped ZrO₂. In pursuit of augmenting the research area of d^0 ferromagnetism, we have endeavoured a study on the crystal structure and magnetic properties of Ag-doped ZrO₂ compounds. We have chosen to prepare materials in bulk form at equilibrium conditions to diminish the uncertainties in fabrications and any inaccuracies in characterization.

2. Experimental Details

The polycrystalline samples of Zr_{1-x}Ag_xO₂ (x=0, 0.02, 0.04, 0.06 and 0.08) were prepared by solid-state reaction route. We used high-purity ZrO₂ and AgNO₃ as the starting materials for synthesis of our samples. The maximum amount of any kind of trace magnetic impurities in the starting materials was found to be less than 0.9 % ppm as mentioned by the supplier

ICP chemical analyses report. Pre-sintering of the prepared samples was performed in powder form at various temperatures, i.e. 200⁰C and 300⁰C for about 20 hours at each temperature. The samples were further annealed in pallet form at 500⁰C for 30 hrs. One sample of Zr_{0.94}Ag_{0.06}O₂ was prepared at 1350⁰C to study the influence of sintering temperature. The crystal structure of the prepared samples was checked using X-ray diffractometer. The temperature (T) variation of magnetization (M) and, magnetization versus magnetic field (H) measurements were carried out using commercial SQUID magnetometer and vibrating sample magnetometer (VSM). The magnetic measurements were done with utmost care and repeated two times with different pieces of samples to guarantee the reproducibility of results

3. Results and Discussion

The crystal structure and phase purity of all Ag-doped ZrO₂ compounds were checked by X-ray diffractometer and the XRD patterns of these compounds are shown in Figure 1. All the XRD peaks could be indexed to monoclinic symmetry of ZrO₂. Within the instrumental limit of the X-ray diffractometer, the XRD patterns also indicate that samples are formed in single phase and no secondary phase is present. To gain insight into various crystal structural parameters, the refinement of the XRD patterns was performed with the help of the Fullprof program by employing the Rietveld refinement technique [51]. Figure 2 shows the typical Rietveld refinement of XRD patterns for ZrO₂ and Zr_{0.94}Ag_{0.06}O₂ compounds. It is seen that the experimental XRD data matches perfectly with the Rietveld software calculated XRD data. Figure 3 presents the variation of lattice parameters ‘a’ ‘b’, ‘c’ and cell volume (V) for Zr_{1-x}Ag_xO₂ (x=0, 0.02, 0.04, 0.06 and 0.08) compounds. For pure ZrO₂ compound, the lattice parameters are estimated to be a=5.1468Å, b= 5.2041Å, c=5.3198 Å and they are found to be comparable with the values reported in other work [21]. The lattice parameters and unit cell volume of the all Ag-doped ZrO₂ compounds are found to increase with the increase of Ag-doping. Doping of bigger Ag¹⁺ ion (ionic radii of 1.15 Å) into the Zr⁴⁺ (ionic radii of 0.72 Å) is the likely cause of expansion of the lattice parameters and cell volume.

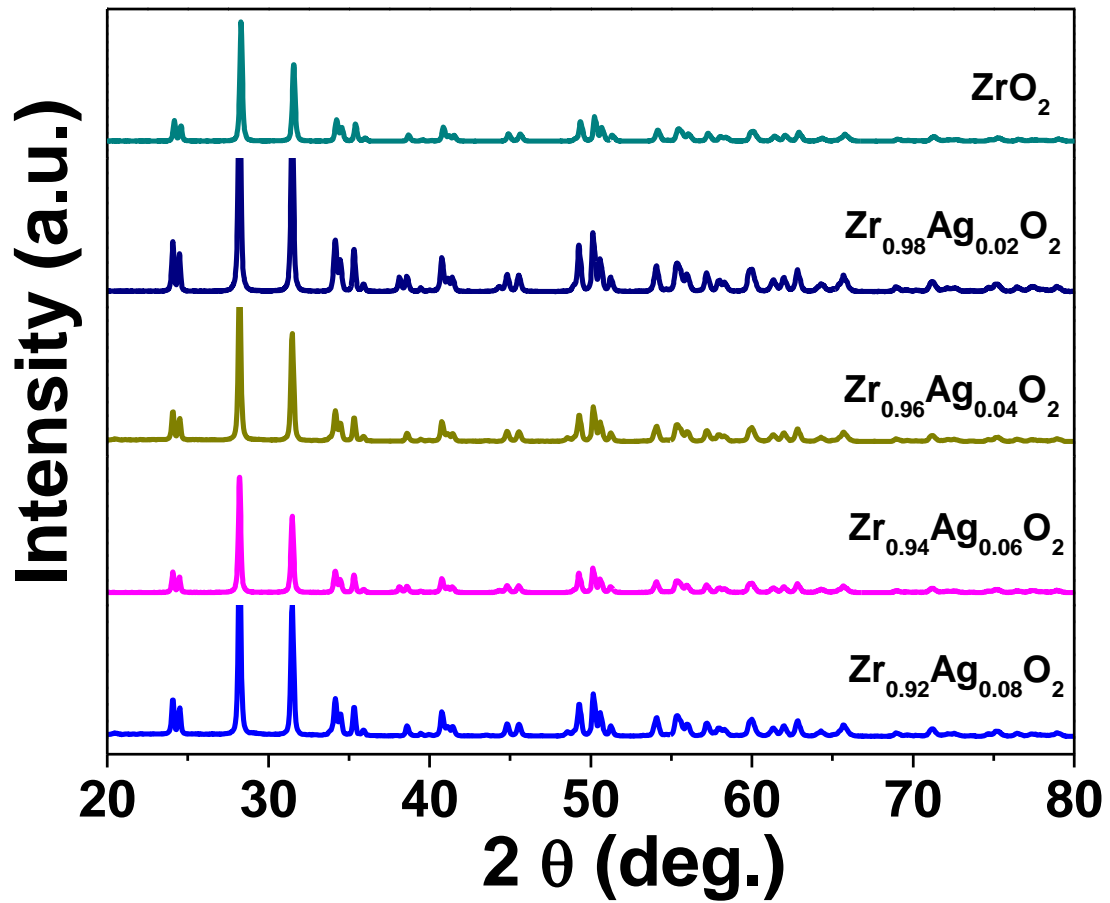


Figure 1: XRD patterns of $\text{Zr}_{1-x}\text{Ag}_x\text{O}_2$ ($x=0, 0.02, 0.04, 0.06$ & 0.08) compounds.

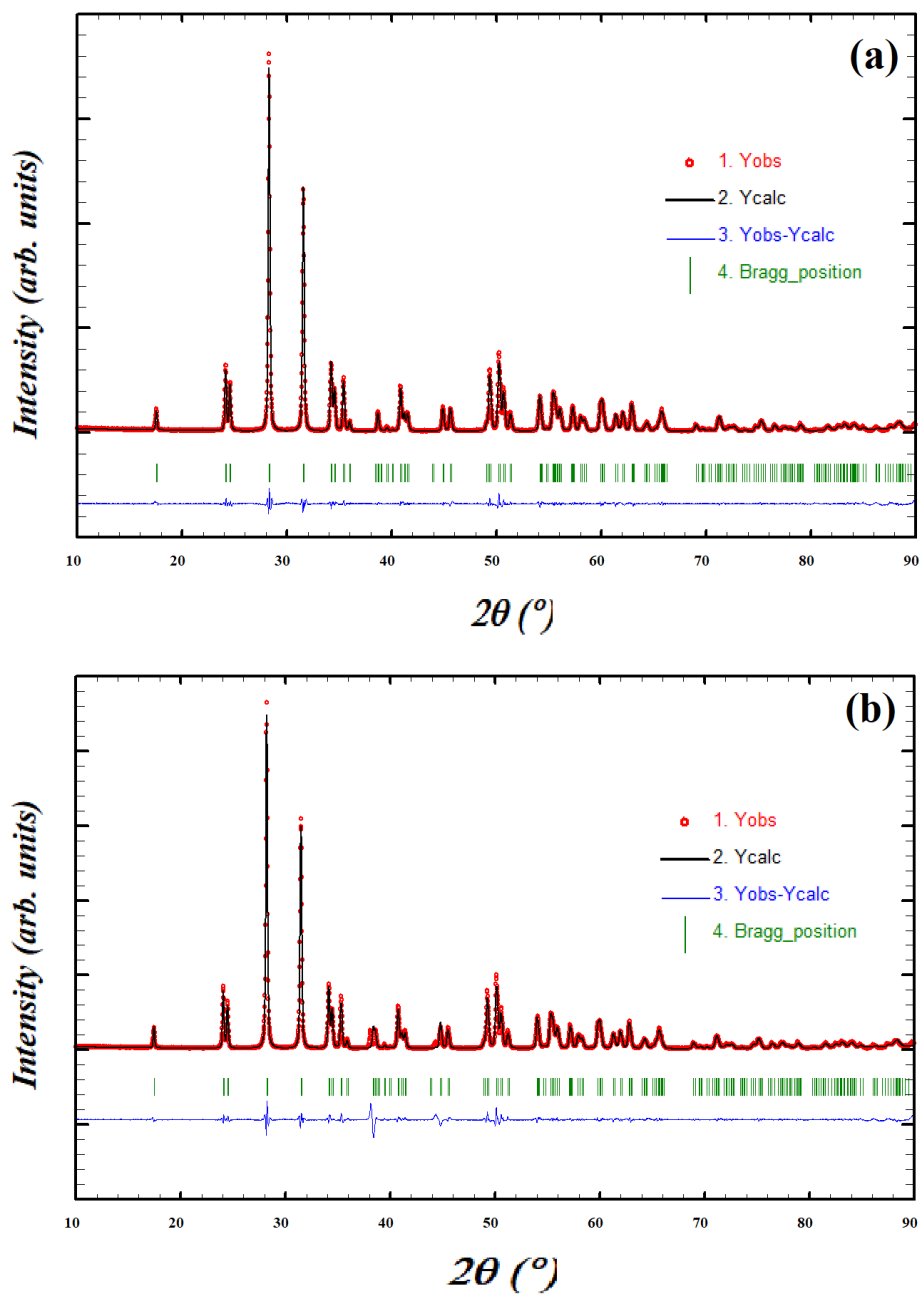


Figure 2: Refinement of XRD patterns for (a) ZrO_2 (b) $Zr_{0.94}Ag_{0.06}O_2$ compounds, obtained with the help of the Fullprof program by employing the Rietveld refinement technique.

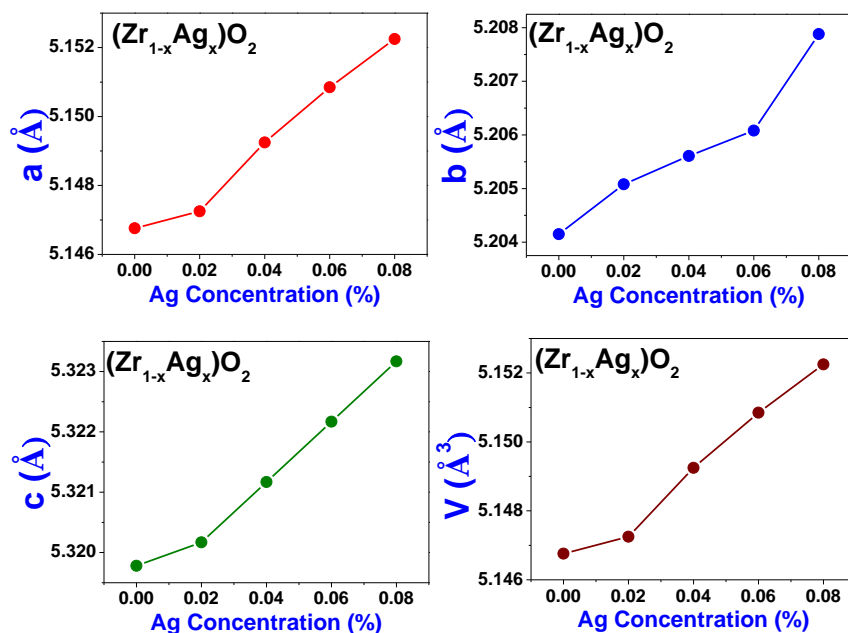


Figure 3: Variation of lattice parameters ‘a’ ‘b’, ‘c’ and cell volume (V) for $Zr_{1-x}Ag_xO_2$ ($x=0, 0.02, 0.04, 0.06$ and 0.08) compounds.

In order to explore the magnetic properties of these prepared compounds, the zero-field cooled (ZFC) magnetization curves as a function of temperature for all Ag-doped ZrO_2 compounds were measured under an applied field of 500 Oe using SQUID magnetometer. The temperature variation of magnetization as a function of temperature i.e. M-T curve for pure ZrO_2 compound shows a paramagnetic behavior of the sample, as depicted in Figure 4(a). In addition, the magnetization versus applied field measurement performed at 3K for pure ZrO_2 again indicates the paramagnetic nature of the compound as shown in figure 4(b). Thus, pure ZrO_2 compound is found to exhibit paramagnetic behavior. Figure 5 presents the temperature variation of magnetization curves for all Ag-doped ZrO_2 compounds. It is observed that the magnetization decreases with the increase of temperature throughout the measured temperature range for $Zr_{0.98}Ag_{0.02}O_2$ compound. However, higher Ag-doped compounds i.e. $Zr_{0.96}Ag_{0.04}O_2$ and $Zr_{0.94}Ag_{0.06}O_2$ compounds are found to exhibit a clear ferromagnetic to paramagnetic transition. Moreover, $Zr_{0.92}Ag_{0.08}O_2$ compound exhibits interesting feature. The measurement of ZFC M-T curve for this sample show that there is a low temperature antiferromagnetic (AFM) transition at ~ 55 K, followed by weak ferromagnetic to paramagnetic transition at ~ 165 K (as shown in the inset of Figure 5d). It indicates that weak ferromagnetic phase is superimposed with the dominating antiferromagnetic phase. To get further insight into the magnetic property of $Zr_{0.92}Ag_{0.08}O_2$

compound, we have measured the M-T curve under field cooled (FC) condition along with ZFC condition and the data are presented in Figure 5 (d). The measurements of ZFC and FC magnetization data for this sample indicate that ZFC and FC M-T curves coincide at low temperature and the magnitude of magnetization at AFM transition temperature of under FC condition has increased, indicating an antiferromagnetic interaction in the matrix. Similar observations have been reported in Fe-doped SnO₂ compounds [52]. To determine the ferromagnetic (FM) transition temperature (T_C), peaks observed in |dM/dT| versus temperature plot have been used. Here, T_C value was taken as the minimum of |dM/dT| plot and fitting the curve with a Gaussian function. Typical plots of |dM/dT| versus temperature for x = 0.04 and 0.08 samples are shown in Figure 6. The T_C values are obtained as 108.2, 192.4 and 172.6 K for x = 0.04, 0.06 and 0.08 samples respectively. Thus, the introduction of Ag in ZrO₂ gives rise to increase in ferromagnetic T_C. Moreover, the magnitude of magnetization is found to increase with Ag concentration in addition to increase in the FM T_C. The decrease of magnetization for x=0.08 sample is due to presence of competing AFM interaction. For the estimation of Curie-temperature (θ_C), the paramagnetic region of ZFC M-T curve was analyzed using Curie-Weiss law, $\chi = C_0x/(T - \theta_C)$. Typical plots of 1/χ_{dc} versus temperature for x= 0.02, 0.04 and 0.08 samples are shown in Figure 7 along with Curie-Weiss law fitting and the estimated Curie-temperature (θ_C) values are listed in Table 1. The value of Curie-temperature (θ_C) is found to be 28.7, 126.8 and 163.2 K for x=0.02, 0.04 and 0.08 samples respectively. The positive values of θ_C indicate the FM interaction. The difference between T_C and θ_C are mainly due to the observed broad magnetic transition. We could not fit data for x=0.06 sample due to non-availability of sufficient data in the paramagnetic region. For calculating effective paramagnetic moment (μ_{eff}), the relation, $\mu_{eff} = \sqrt{3k_B C_0 x / N \mu_0 \mu_B^2}$ was used and the values were found to be 1.40 μ_B/Ag ion, 2.27 μ_B/Ag ion and 0.16 μ_B/Ag ion for 2, 4 and 8 % Ag-doped samples respectively.

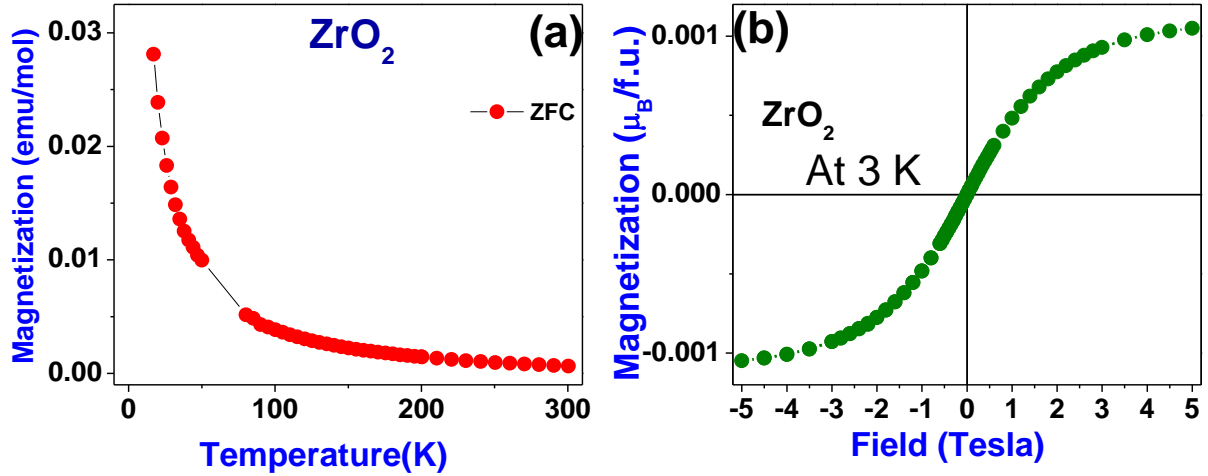


Figure 4:(a) M-T curve for pure ZrO_2 under a field of 0.05 T and (b) M-H loop obtained at 3 K for the ZrO_2 sample.

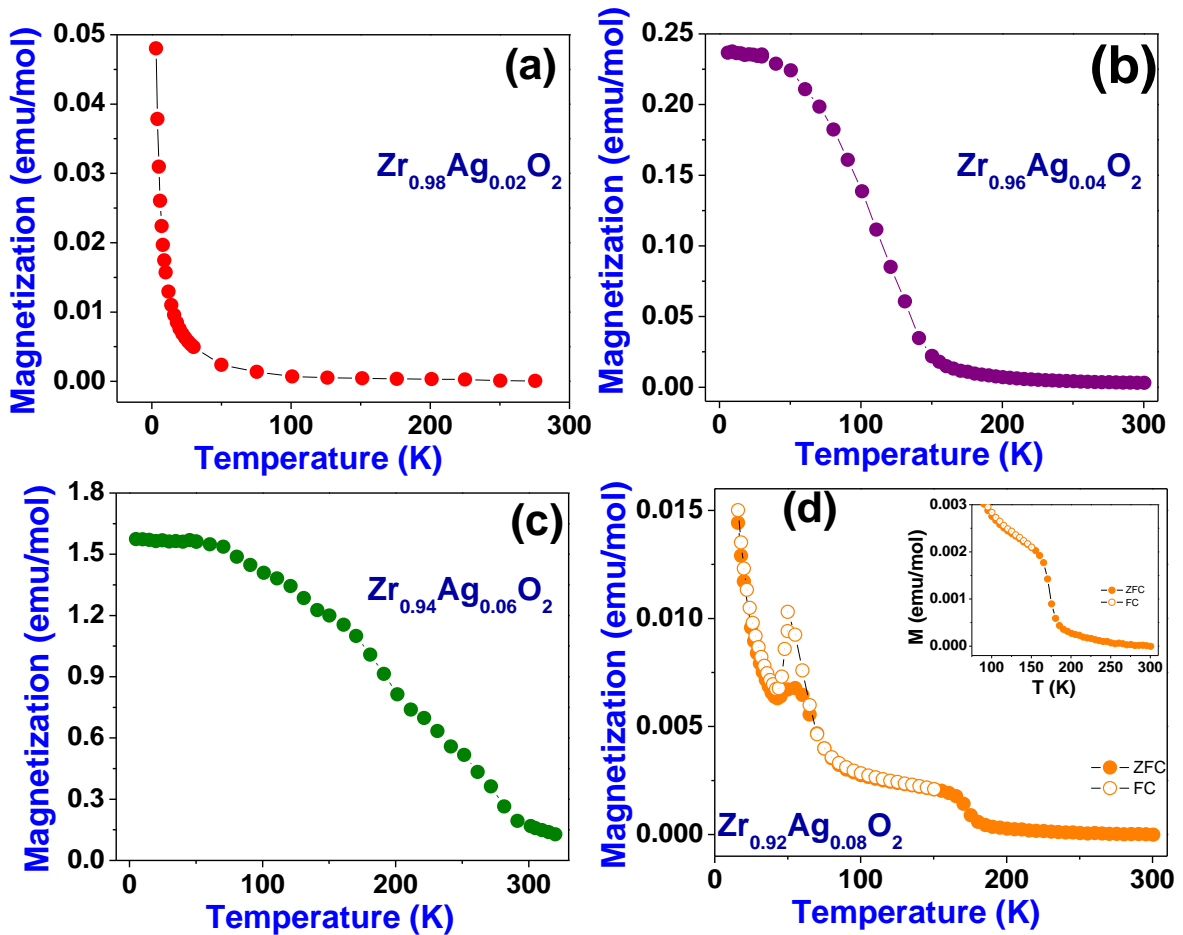


Figure 5:(a) Temperature variation of magnetization of Ag-doped ZrO_2 samples measured under an applied field of 0.05 T field.

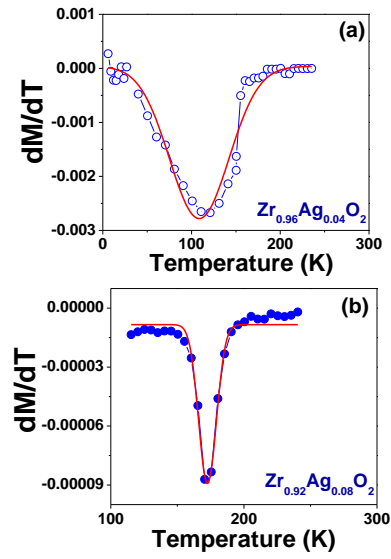


Figure 6: Temperature variation of $|dM/dT|$ for $Zr_{0.96}Ag_{0.04}O_2$ and $Zr_{0.92}Ag_{0.08}O_2$.

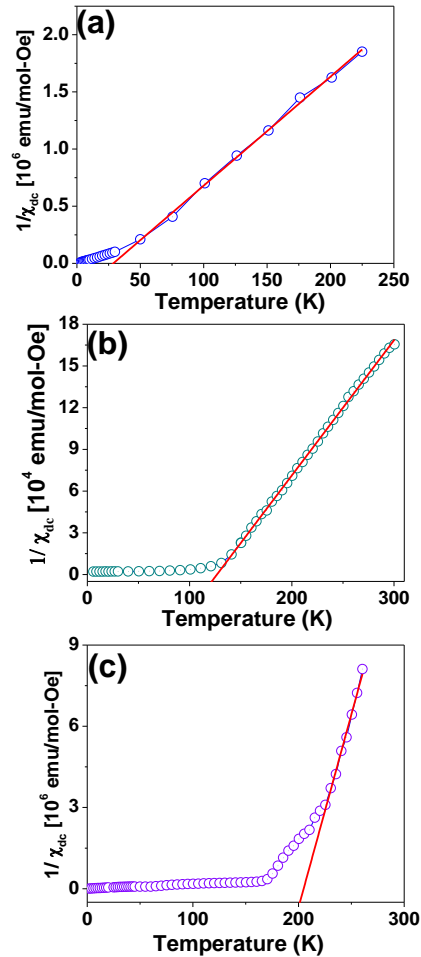


Figure 7: Temperature variation of inverse of susceptibility ($1/\chi_{dc}$) for $Zr_{1-x}Ag_xO_2$ with (a) $x=0.02$ (b) $x=0.04$ and (c) $x=0.08$ compounds. Solid lines represent fit to the Curie-Weiss law.

The field variation of magnetization measurements i.e. M - H curves at 3 K were performed for all Ag-doped ZrO_2 compounds and they are shown in Figure 8. From the curves, it is observed that the magnetization of these samples gets saturated at relatively larger applied field. One can see that the samples show a clear ferromagnetic behaviour at 3 K. The value of saturation magnetization (M_s) is found to be 0.003, 0.006, 0.009 and 0.004 μ_B/Ag ion for $x= 0.02, 0.04, 0.06$ and, 0.08 respectively. The decrease in M_s value for $x=0.08$ sample is possibly due to the presence of AFM interaction in the sample. Although, $Zr_{0.98}Ag_{0.02}O_2$ does not clearly exhibit any hysteresis loop but, higher Ag doped ZrO_2 compounds exhibit hysteresis loops with a coercivity of around 1350 Oe.

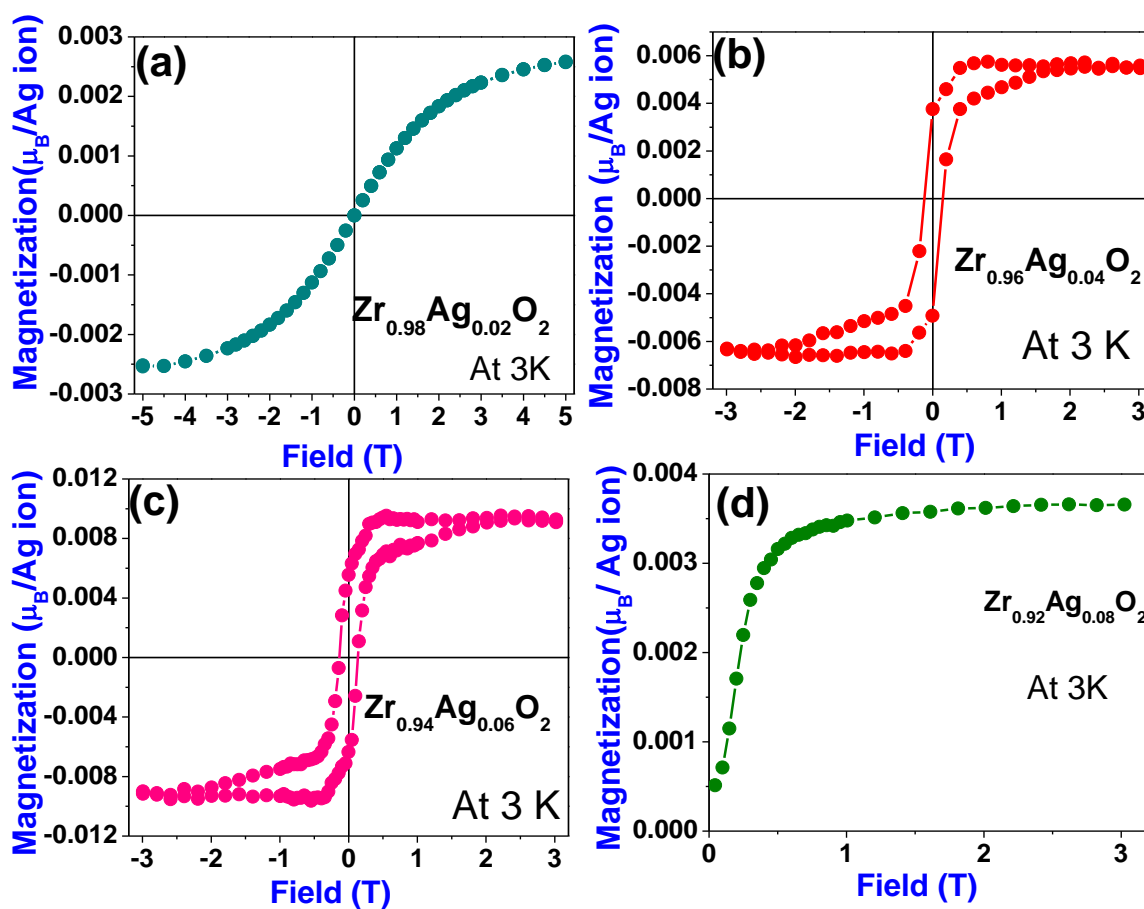


Figure 8: Field variation of magnetization for $Zr_{1-x}Ag_xO_2$ ($x=0.02, 0.04, 0.06$ and 0.08) compounds measured at 3 K.

Table 1: Parameters obtained from ZFC magnetization measurements of $Zr_{1-x}Ag_xO_2$ ($x=0, 0.02, 0.04, 0.06, 0.08$) compounds. Here, T_C is ferromagnetic transition temperature. θ_C and μ_{eff} (μ_B/ion) are Curie temperature and experimental effective magnetic moment respectively, obtained from the Curie-Weiss law fit of susceptibility data.

Sample/ Parameters	x=0.02	x=0.04	x=0.06	x=0.08
T_C (K)	--	108.6	192.4	172.6
θ_C (K)	28.7	126.8	--	163.2
μ_{eff} (μ_B/Ag ion)	1.40	2.27	--	0.16
M_S (μ_B/Ag ion)	0.003	0.006	0.009	0.004

To study the influence of sintering temperature on the magnetic property, one sample of $Zr_{0.94}Ag_{0.06}O_2$ was prepared by sintering it at 1350°C. The crystal structure from XRD patterns indicates that sample has been crystallized in monoclinic symmetry of ZrO_2 (not shown). Figure 9 shows the M-T and M-H (at 3K) curves measured for this sample. The measurement of M-T curve, as shown in Figure 9(a) indicates that it exhibits paramagnetic behaviour and it is further corroborated by M-H curve, as shown in Figure 9 (b). Moreover, from the M-H curve, it is observed that the value of magnetization decreases with increase in the sintering temperature. The saturation magnetization is two times larger for the sample prepared at 500 °C, as compared with the sample prepared at 1350 °C. These results suggest that oxygen vacancies present in the sample prepared at lower temperature lead to ferromagnetism, which get diminished in the sample prepared at high-temperature. High-temperature preparation results in the destruction of the ferromagnetic ordering and reduced magnetic moment, possibly due to decrease in oxygen vacancies. Similar observation was made for Cu doped TiO_2 [31-32].

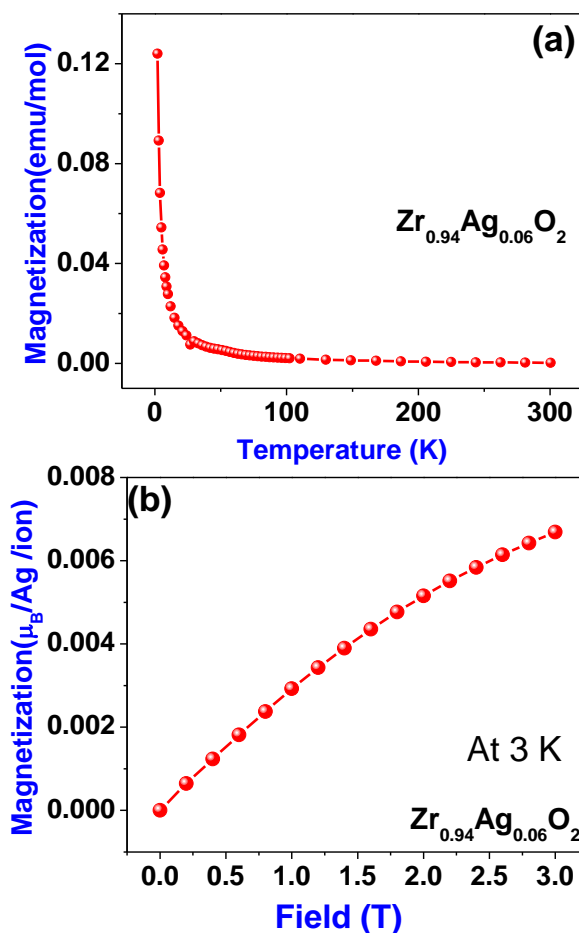


Figure 9: (a) Temperature variation of magnetization and (b) Magnetization versus field variation at 3K of $Zr_{0.94}Ag_{0.06}O_2$ compound, prepared at $1350^{\circ}C$.

Let us summarize the magnetism observed in these samples. The measurement of magnetic properties of these compounds indicates that pure ZrO_2 compound exhibit paramagnetic behavior, which is unlike few previous reports where ferromagnetism was observed in pure ZrO_2 [42-43]. However, the Ag-doped ZrO_2 compounds exhibits ferromagnetic to paramagnetic transition and FM transition temperature was found to increase with the increase of Ag concentration. Thus, the introduction of Ag in ZrO_2 gives rise to increase in ferromagnetic T_C . Moreover, the magnitude of magnetization is found to increase with Ag concentration in addition to increase in the FM T_C . When we consider the effect of sintering temperature on the magnetic property, the sample prepared at lower temperature is found to be ferromagnetic and this is due to the vacancies present therein.

It is an established fact in the realm of the physics and chemistry of solids that that ions substitute for one-another in structures if the charges and sizes are similar, it is usually evident from a systematic cell parameter change. In the case of a direct cationic substitution, theoretical model study [21] and first principle approach study in ZrO_2 [16, 26] and

observation of d^0 magnetism in K doped SnO₂ [34] have demonstrated that three physical parameters are essential to explain induced d^0 magnetism: (i) the position of the induced impurity band (ii) the density of carrier per defect and (ii) the electrons-electrons correlations [21, 34]. In present study, ZrO₂ has 6-coordinate Zr⁴⁺ and the replacement of Zr⁴⁺ by Ag¹⁺ will produce three holes. To retain charge neutrality, it is possible that more defect species such as oxygen vacancies (V_o) are created in ZrO₂ structure as oxidation states of Ag¹⁺ is lower in comparison to Zr⁴⁺. A vacancy induces local magnetic moments on the neighboring oxygen atoms which then interact with extended exchange couplings they interact ferromagnetically via O. Furthermore, it should be noted that we have not observed any secondary phase from the crystal structure and thus the observed ferromagnetism has intrinsic nature. It should be noted that the tetragonal or cubic symmetry of ZrO₂ is not absolutely necessary to obtain d^0 ferromagnetism.

4. Conclusion

To conclude, polycrystalline samples of Zr_{1-x}Ag_xO₂ (x=0, 0.02, 0.04, 0.06 and 0.08) were prepared by solid-state reaction route. All the prepared compounds are found to crystallize in monoclinic symmetry of ZrO₂ with typical lattice parameters of a=5.1468Å, b= 5.2041Å, c=5.3198 Å for pure ZrO₂ compound. The measurement of magnetic properties of these compounds indicates that pure ZrO₂ compound exhibits paramagnetic behavior. However, the Ag-doped ZrO₂ compounds exhibit ferromagnetic to paramagnetic transition. The Curie temperature (θ_C) was found to increase from 28.7K for x=0.02 to 173.2 K for x= 0.08 doped ZrO₂. Thus, the introduction of Ag in ZrO₂ induces ferromagnetism with a large θ_C . The measurement of hysteresis curves indicates that Ag doped ZrO₂ compounds exhibit hysteresis loops with a coercivity of around 1350 Oe. In this study, increase in Ag concentration resulted increase in the value of saturation magnetization (M_S). The maximum value of M_S was found to be 0.009 μ_B /Ag ion for x= 0.06 sample. The study of influence of sintering temperature suggests that ferromagnetism observed in the sample prepared at low temperature (500°C) is possibly due to oxygen vacancies present in the sample. The sintering of sample at high temperature (1350°C) diminishes the ferromagnetism and it leads to paramagnetic behaviour.

Acknowledgements

This research did not receive any specific grant from funding agencies in the public, commercial, or not-for-profit sectors.

References:

- [1] H. Ohno, Making Nonmagnetic Semiconductors Ferromagnetic, *Science* 281 (1998) 951-956. <https://doi.org/10.1126/science.281.5379.951>.
- [2] S. A. Wolf, D. D. Awschalom, R. A. Buhrman, J. M. Daughton, S. V. Molnar, M. L. Roukes, A. Y. Chtcheljanova and D. M. Treger, Spintronics: A Spin-Based Electronics Vision for the Future, *Science* 294 (2001) 1488–1495. <https://doi.org/10.1126/science.1065389>.
- [3] J. K. Furdyna, Diluted magnetic semiconductors, *J. Appl. Phys.* 64 (1988) R29–R64. <https://doi.org/10.1063/1.341700>.
- [4] S.B. Ogale, R.J. Choudhary, J.P. Buban, S.E. Lofland, S.R. Shinde, S.N. Kale, V.N. Kulkarni, J. Higgins, C. Lanci, J.R. Simpson, N.D. Browning, S. Das Sarma, H.D. Drew, R.L. Greene, T. Venkatesan, High Temperature Ferromagnetism with a Giant Magnetic Moment in Transparent Co-doped SnO_{2-δ}, *Phys. Rev. Lett.* 91 (2003). <https://doi.org/10.1103/physrevlett.91.077205>.
- [5] X.L. Wang, Z.X. Dai, Z. Zeng, Search for ferromagnetism in SnO₂ doped with transition metals (V, Mn, Fe, and Co), *J. Phys.: Condens. Matter* 20 (2008) 45214. <https://doi.org/10.1088/0953-8984/20/04/045214>.
- [6] S. K. Srivastava, R. Brahma, S. Datta, S. Guha, Aakansha, S. S. Baro, B. Narzary, D. R. Basumatary, M. Kar, S. Ravi, Effect of (Ni-Ag) co-doping on crystal structure and magnetic Property of SnO₂, *Mater. Res. Express* 6 (2019) 126107. <https://doi.org/10.1088/2053-1591/ab58b1>.
- [7] P. Sharma, A. Gupta, K. V. Rao, F. J. Owens, R. Sharma, R. Ahuja, J M Osorio Guillen, B. Johansson and G. A. Gehring, Ferromagnetism Above Room Temperature in Bulk and Transparent Thin Films of Mn-doped ZnO, *Nature Mater.* 2 10 (2003): 673-677. <https://doi.org/10.1038/nmat984>.
- [8] M. Subramanian, P. Thakur, M. Tanemura, T. Hihara, V. Ganesan, T. Soga, K. H. Chae, R. Jayavel and T. Jimbo, Intrinsic ferromagnetism and magnetic anisotropy in Gd-doped ZnO thin films synthesized by pulsed spray pyrolysis method, *J. Appl. Phys.* 108 (2010) 53904. <https://doi.org/10.1063/1.3475992>.
- [9] J.D. Bryan, S.M. Heald, S.A. Chambers, D.R. Gamelin, Strong Room-Temperature Ferromagnetism in Co²⁺-Doped TiO₂ Made from Colloidal Nanocrystals, *J. Am. Chem. Soc.* 126 (2004) 11640-11647. <https://doi.org/10.1021/ja047381r>.

- [10] A. Punnoose and J. Hays, Possible metamagnetic origin of ferromagnetism in transition-metal-doped SnO₂, *J. Appl. Phys.* **97** (2005) 10D321. <https://doi.org/10.1063/1.1853331>.
- [11] S. K. Srivastava, P. Lejay, B. Barbara, S. Pailhès, and G. Bouzerar, “Absence of ferromagnetism in Mn-doped tetragonal zirconia” *J. Appl. Phys.* **110**, (2011) 043929. <https://doi.org/10.1063/1.3626788>.
- [12] S. K. Srivastava, Magnetic Property of Mn-Doped Monoclinic ZrO₂ Compounds, *J. Supercond. Nov. Magn.* (2020). <https://doi.org/10.1007/s10948-020-05522-1>.
- [13] T. Dietl, A ten-year perspective on dilute magnetic semiconductors and oxides, *Nature Mater.* **9** (2010) 965–974. <https://doi.org/10.1038/nmat2898>.
- [14] M. Venkatesan, C.B. Fitzgerald, J.M.D. Coey, Unexpected magnetism in a dielectric oxide, *Nature* **430** (2004) 630–630. <https://doi.org/10.1038/430630a>.
- [15] J. Osorio-Guillen, S. Lany, S.V. Barabash, A. Zunger, Magnetism without Magnetic Ions: Percolation, Exchange, and Formation Energies of Magnetism-Promoting Intrinsic Defects in CaO, *Phys. Rev. Lett.* **96** (2006). <https://doi.org/10.1103/physrevlett.96.107203>.
- [16] F. Máca, J. Kudrnovský, V. Drchal, G. Bouzerar, Magnetism without magnetic impurities in ZrO₂ oxide, *Appl. Phys. Lett.* **92** (2008) 212503. <https://doi.org/10.1063/1.2936858>.
- [17] J. P. Singh and K. H. Chae, d⁰ Ferromagnetism of Magnesium Oxide, *Condens. Matter* **2** (2017) 36. <https://doi.org/10.3390/condmat2040036>.
- [18] H. Peng, J. Li, S.S. Li, J.B. Xia, Possible origin of ferromagnetism in undoped anataseTiO₂, *Phys. Rev. B* **79** (2009). <https://doi.org/10.1103/physrevb.79.092411>.
- [19] S. Ning, P. Zhan, Q. Xie, Z. Li, Z. Zhang, Room-temperature ferromagnetism in undoped ZrO₂ thin films, *J. Phys. D Appl. Phys.* **46** (2013) 445004. <https://doi.org/10.1088/0022-3727/46/44/445004>.
- [20] C. Das Pemmaraju, S. Sanvito, Ferromagnetism Driven by Intrinsic Point Defects in HfO₂, *Phys. Rev. Lett.* **94** (2005). <https://doi.org/10.1103/physrevlett.94.217205>
- [21] G. Bouzerar, T. Ziman, Model for Vacancy-Induced d⁰ Ferromagnetism in Oxide Compounds, *Phys. Rev. Lett.* **96** (2006). <https://doi.org/10.1103/physrevlett.96.207602>.
- [22] W. Zhou, L. Liu, P. Wu, Nonmagnetic impurities induced magnetism in SnO₂, *J. Magn. Mater.* **321** (2009) 3356–3359. <https://doi.org/10.1016/j.jmmm.2009.06.016>.

- [23] W.-Z. Xiao, L.-L. Wang, L. Xu, X.-F. Li, H.-Q. Deng, First-principles study of magnetic properties in Ag-doped SnO₂, *Phys. Status Solidi B* 248 (2011) 1961–1966. <https://doi.org/10.1002/pssb.201046567>.
- [24] C.W. Zhang, S.S. Yan, First-principles study on ferromagnetism in Mg-doped SnO₂, *Appl. Phys. Lett.* 95 (2009) 232108. <https://doi.org/10.1063/1.3272674>.
- [25] J. G. Tao, L. X. Guan, J. S. Pan, C. H. A. Huan, L. Wang, J. L. Kuo, Possible room temperature ferromagnetism of Li-doped anatase TiO₂: A first-principles study, *Phys. Lett. A*. 374 (2010) 4451–4454. <https://doi.org/10.1016/j.physleta.2010.08.074>.
- [26] F. Maca, J. Kudrnovsky, V. Drchal, G. Bouzerar, Magnetism without magnetic impurities in oxides ZrO₂ and TiO₂, *Philos. Mag.* 88 (2008) 2755–2764. <https://doi.org/10.1080/14786430802342584>.
- [27] J. Osorio-Guillén, S. Lany, and A. Zunger, Atomic Control of Conductivity versus Ferromagnetism in Wide-Gap Oxides via Selective Doping: V, Nb, Ta in Anatase TiO₂ *Phys. Rev. Lett.* 100 (2008). <https://doi.org/10.1103/physrevlett.100.036601>.
- [28] S. Chawla, K. Jayanthi, R.K. Kotnala, Room-temperature ferromagnetism in Li-doped p-type luminescent ZnO nanorods, *Phys. Rev. B* 79 (2009). <https://doi.org/10.1103/physrevb.79.125204>.
- [29] S. Chawla, K. Jayanthi, R.K. Kotnala, High temperature carrier controlled ferromagnetism in alkali doped ZnO nanorods, *J. Appl. Phys.* 106 (2009) 113923. <https://doi.org/10.1063/1.3261722>.
- [30] J.B. Yi, C.C. Lim, G.Z. Xing, H.M. Fan, L.H. Van, S.L. Huang, K.S. Yang, X.L. Huang, X.B. Qin, B.Y. Wang, T. Wu, L. Wang, H.T. Zhang, X.Y. Gao, T. Liu, A.T.S. Wee, Y.P. Feng, J. Ding, Ferromagnetism in Dilute Magnetic Semiconductors through Defect Engineering: Li-Doped ZnO, *Phys. Rev. Lett.* 104 (2010). <https://doi.org/10.1103/physrevlett.104.137201>.
- [31] D. L. Hou, H. J. Meng, L. Y Jia, X. J. Ye, H. J. Zhou, X. L. Li, Impurity concentration study on ferromagnetism in Cu-doped TiO₂ thin films, *EPL* 78 (2007) 67001. <https://doi.org/10.1209/0295-5075/78/67001>.
- [32] S. Duhalde, M.F. Vignolo, F. Golmar, C. Chilotte, C.E.R. Torres, L.A. Errico, A.F. Cabrera, M. Rentería, F.H. Sánchez, M. Weissmann, Appearance of room-temperature ferromagnetism in Cu-doped TiO_{2-δ} films, *Phys. Rev. B* 72 (2005). <https://doi.org/10.1103/physrevb.72.161313>.

- [33] X.J. Ye, W. Zhong, M.H. Xu, X.S. Qi, C.T. Au, Y.W. Du, The magnetic property of carbon-doped TiO₂, *Phys. Lett. A* 373 (2009) 3684–3687. <https://doi.org/10.1016/j.physleta.2009.08.007>.
- [34] S. K. Srivastava, P. Lejay, B. Barbara, S. Pailhès, V. Madigou, and G. Bouzerar, Possible room-temperature ferromagnetism in K-doped SnO₂: X-ray diffraction and high-resolution transmission electron microscopy study, *Phys. Rev. B* 82 (2010). <https://doi.org/10.1103/physrevb.82.193203>.
- [35] S. K. Srivastava, P. Lejay, A. Hadj-Azzem, G. Bouzerar, Non-magnetic Impurity Induced Magnetism in Li-Doped SnO₂ Nanoparticles, *J. Supercond. Nov. Magn.* 27 (2013) 487–492. <https://doi.org/10.1007/s10948-013-2287-0>.
- [36] S. K. Srivastava, P. Lejay, B. Barbara, O. Boisron, S. Pailhès and G. Bouzerar, Non-magnetic impurity induced magnetism in rutile TiO₂:K compounds, *J. Phys.: Condens. Matter* 23 (2011) 442202. <https://doi.org/10.1088/0953-8984/23/44/442202>.
- [37] N. Ali, B. Singh, Z.A. Khan, V. A. R., K. Tarafder, S. Ghosh, Origin of ferromagnetism in Cu-doped ZnO, *Sci. Rep.* 9 (2019). <https://doi.org/10.1038/s41598-019-39660-x>.
- [38] J. Wang, D. Zhou, Y. Li, P. Wu, Experimental and first-principle studies of ferromagnetism in Na-doped SnO₂ nanoparticles, *Vacuum*, 141 (2017) 62–67. <https://doi.org/10.1016/j.vacuum.2017.03.024>.
- [39] D.W. McComb, Bonding and electronic structure in zirconia pseudo polymorphs investigated by electron energy-loss spectroscopy, *Phys. Rev. B* 54 (1996) 7094–7102. <https://doi.org/10.1103/physrevb.54.7094>.
- [40] M. Li, Z. Feng, G. Xiong, P. Ying, Q. Xin, C. Li, Phase Transformation in the Surface Region of Zirconia Detected by UV Raman Spectroscopy, *J. Phys. Chem. B* 105 (2001) 8107–8111. <https://doi.org/10.1021/jp010526l>.
- [41] J.C. Garcia, L.M.R. Scolfaro, A.T. Lino, V.N. Freire, G.A. Farias, C.C. Silva, H. W. Leite Alves, S.C.P. Rodrigues, E.F. da Silva Jr., Structural, electronic, and optical properties of ZrO₂ from ab initio calculations, *J. Appl. Phys.* 100 (2006) 104103. <https://doi.org/10.1063/1.2386967>.
- [42] M. C. Dimri, H. Khanduri, H. Kooskora, M. Kodu, R. Jaaniso, I. Heinmaa, A. Mere, J. Krustok, R. Stern, Room-temperature ferromagnetism in Ca and Mg stabilized cubic zirconia bulk samples and thin films prepared by pulsed laser deposition, *J. Phys. D: Appl. Phys.* 45 (2012) 475003. <https://doi.org/10.1088/0022-3727/45/47/475003>.

- [43] S. Ning, P. Zhan, Q. Xie, Z. Li, Z. Zhang, Room-temperature ferromagnetism in undoped ZrO₂ thin films, *J. Phys. D: Appl. Phys.* 46 (2013) 445004. <https://doi.org/10.1088/0022-3727/46/44/445004>.
- [44] S. Ning, Z. Zhang, Phase-dependent and defect-driven d⁰ ferromagnetism in undoped ZrO₂ thin films, *RSC Adv.* 5 (2015) 3636–3641. <https://doi.org/10.1039/c4ra11924j>.
- [45] Ostanin S, Ernst A, Sandratskii L M, Bruno P, Dane M, Hughes I D, Staunton J B, Hergert W, Mertig I and Kudrnovsky J 2007 *Phys. Rev. Lett.* **98** 016101. <https://doi.org/10.1103/PhysRevLett.98.016101>
- [46] M.A. Wahba, S.M. Yakout, Innovative visible light photocatalytic activity for V-doped ZrO₂ structure: optical, morphological, and magnetic properties, *J. Sol-Gel Sci. Techn.* 92 (2019) 628–640. <https://doi.org/10.1007/s10971-019-05103-2>.
- [47] P. Dutta, M.S. Seehra, Y. Zhang, I. Wender, Nature of magnetism in copper-doped oxides: ZrO₂, TiO₂, MgO, SiO₂, Al₂O₃, and ZnO, *J. Appl. Phys.* 103 (2008) 07D104. <https://doi.org/10.1063/1.2830555>
- [48] S. Bing, L. Li-Feng, H. De-Dong, W. Yi, L. Xiao-Yan, H. Ru-Qi, K. Jin-Feng, Improved Resistive Switching Characteristics of Ag-Doped ZrO₂ Films Fabricated by Sol-Gel Process, *Chin. Phys. Lett.* 25 (2008) 2187–2189. <https://doi.org/10.1088/0256-307x/25/6/072>.
- [49] S. Raj, M. Hattori, M. Ozawa, Preparation and catalytic properties of low content Ag-added ZrO₂ for soot oxidation, *J. Ceram. Soc. Japan* 127 (2019) 818–823. <https://doi.org/10.2109/jcersj2.19121>.
- [50] S. Rani, S. Verma, S. Kumar, Tailoring the structural and optical parameters of zirconia nanoparticles via silver, *Appl. Phys. A* 123 (2017). <https://doi.org/10.1007/s00339-017-1148-2>.
- [51] R. A. Young, *The Rietveld Method* (International Union of Crystallography), reprint first ed., Oxford University Press, New York, 1996
- [52] R. Adhikari, A.K. Das, D. Karmakar, T.V.C. Rao, J. Ghatak, Structure and magnetism of Fe-doped SnO₂ nanoparticles, *Phys. Rev. B* 78 (2008). <https://doi.org/10.1103/physrevb.78.024404>.